Numerical simulation and re-design optimization of impressed current cathodic protection for an offshore platform with biofouling in seawater

Wang Wei

wangwei8038@ouc.edu.cn
School of Materials Science and Engineering,
Ocean University of China,
Qingdao 266100, China

W. Wang, W.-H. Li, L.-Y. Song, W.-J. Fan, X.-J. Liu and H.-B. Zheng, *Materials and Corrosion*, 2018, **69**, 239-250.

Introduction

In this work, a previous off shore platform was protected by an ICCP system with two auxiliary anodes for 10 years.

An auxiliary anode was found lost.

An ICCP re-design for this offshore platform in service was urgently optimized.

Model domain

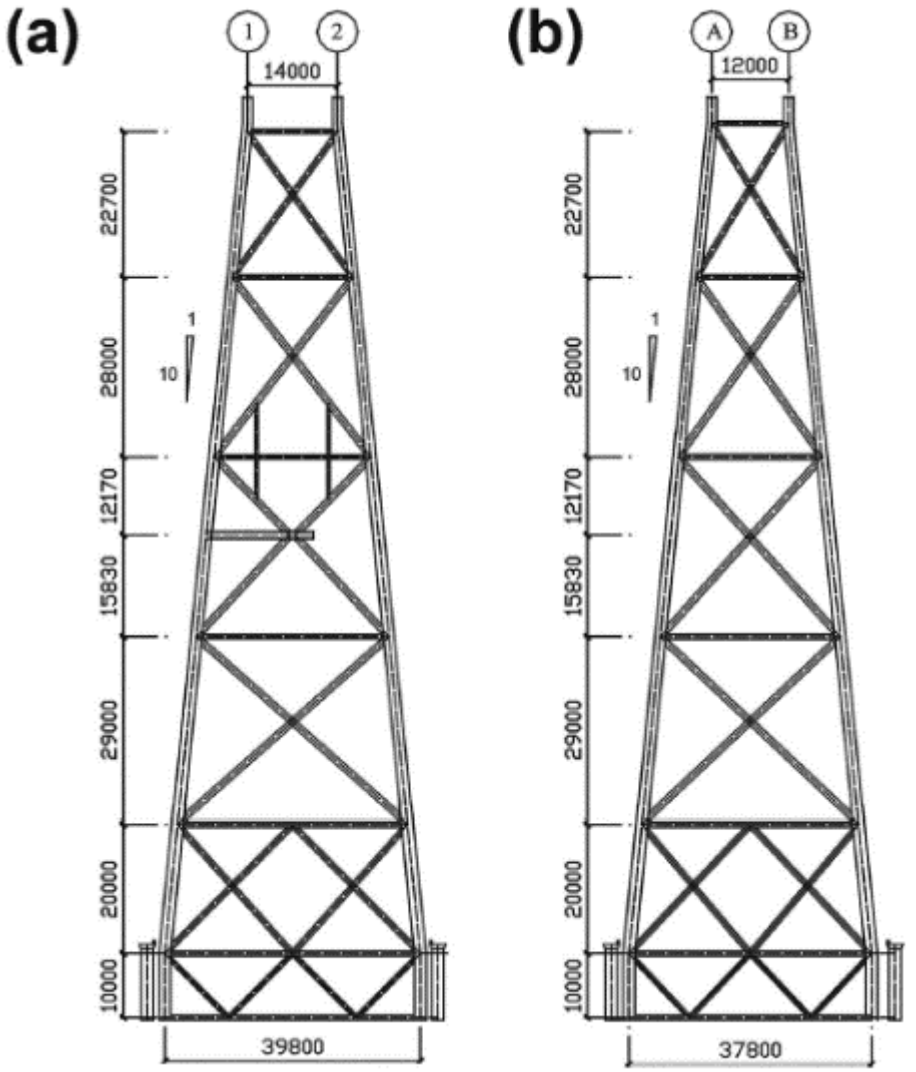

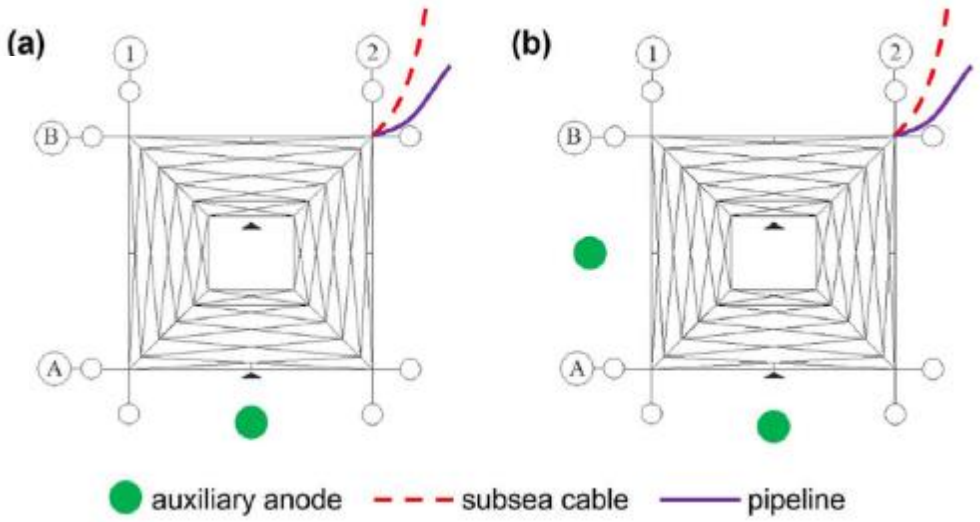

FIGURE 2 Schematic diagram of the placement of optimizing auxiliary anode locations of target zones: (a) one auxiliary anode, (b) two auxiliary anodes.

FIGURE 1 2-D geometries of Row 1–2 (a) and Row A–B (b) of an offshore platform. Dimension: mm

Experiments: FE-SEM pictures

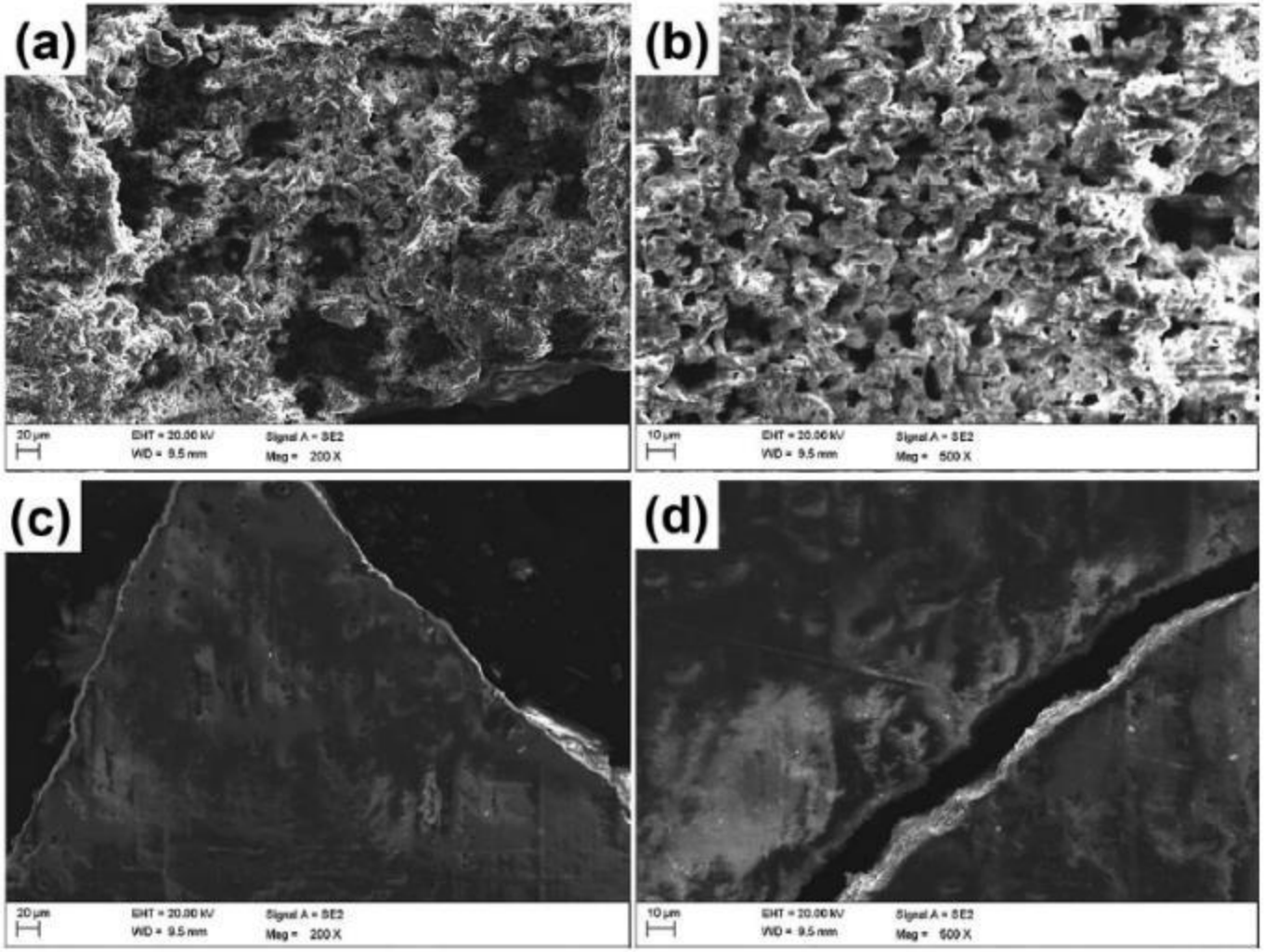

FIGURE 3 FE-SEM pictures of porous loose surfaces of the product and the reverse sides against the Leg A-1 in the depths of 20m (a and c) and 60m (b and d) under seawater.

Experiments: EDS results

Table 1 EDS results of biofouling deposits of the platform leg

Element	C	O	Na	Mg	Al	Si
Atomic%	6.85	71.99	0.84	0.82	0.86	1.61

Element	S	Cl	K	Ca	Fe	Cu
Atomic%	0.54	0.45	0.14	13.92	1.72	0.27

FEM calculations

The potential and current density distributions by FEM simulation are shown in Figure 4b and c.

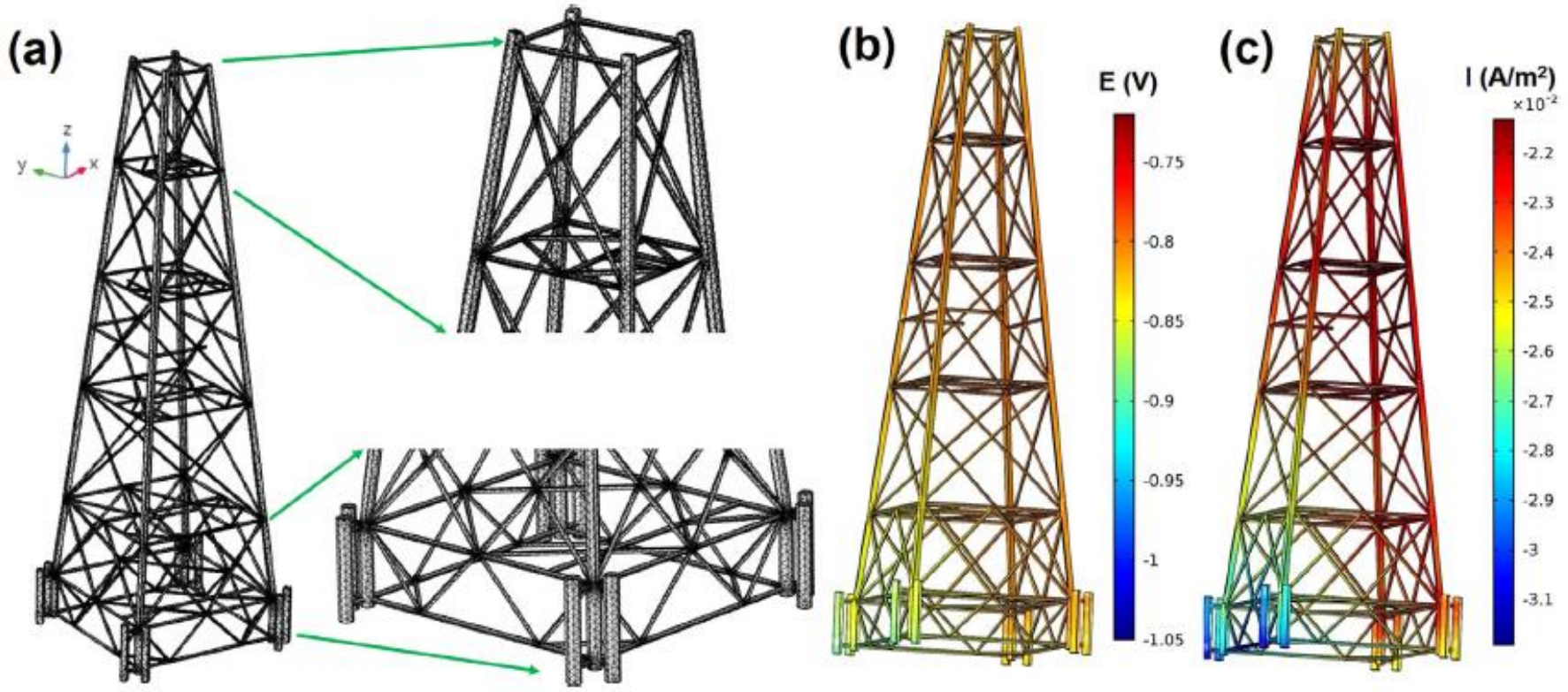

FIGURE 4 (a) 3-D meshes of the offshore platform in simulation environment. The potential (b) and current density (c) distributions calculated by FEM simulation.

Optimization of anode locations

The population standard deviations (σ) was simulated by the following equation:

$$\sigma = \sqrt{\frac{1}{N}\Sigma_{i=1}^{N}(X_i - \mu)^2}$$

The σ values of potential and current density for increasing distance between the anode and the center of the platform had a decreasing trend in Figure 5.

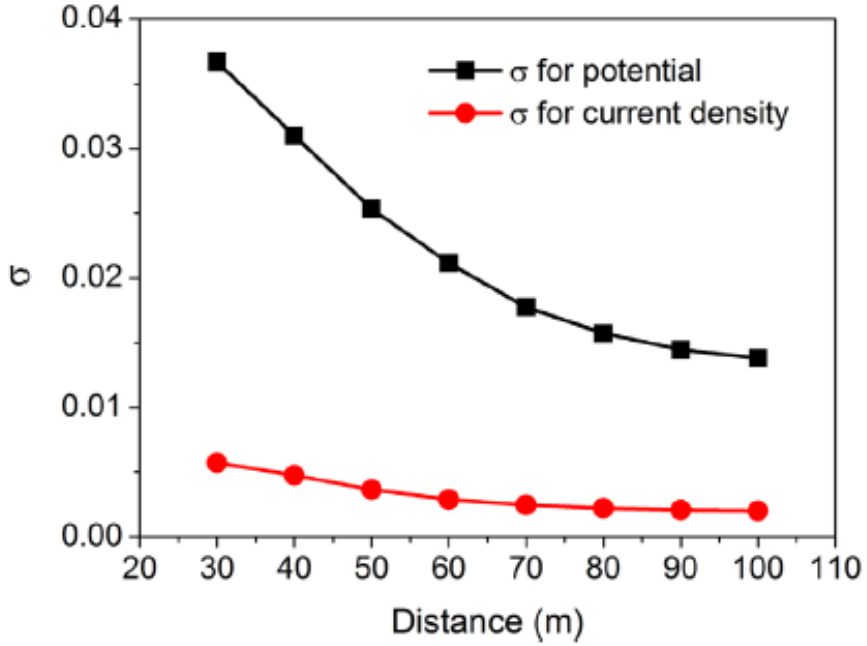

FIGURE 5 Population standard deviations (σ) of potential and current density for different anode locations.

Effect of seawater conductivity

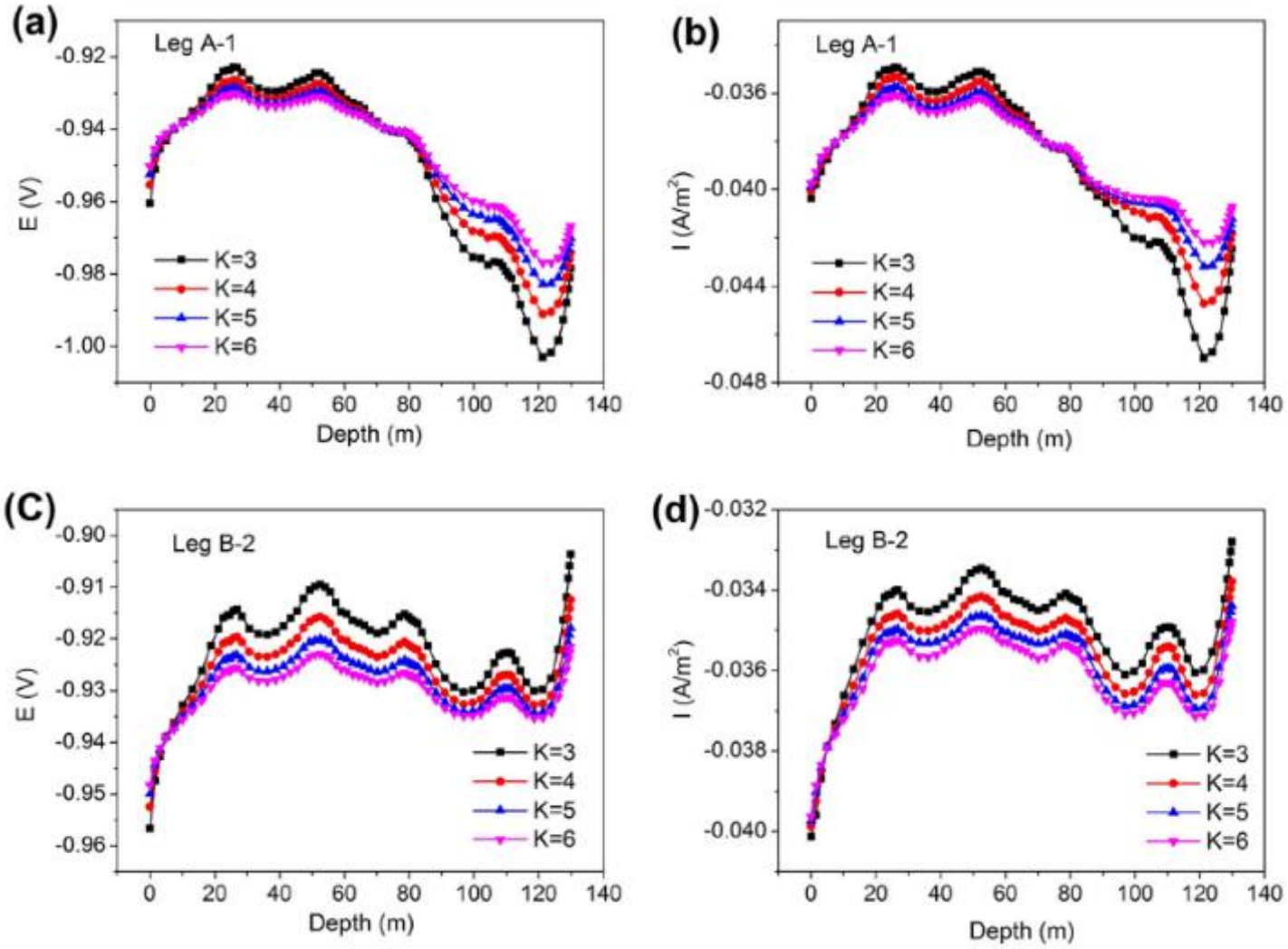

FIGURE 6 Calculated potential and current density distribution of Leg A-1 and Leg B-2 protected by ICCP with different seawater conductivities (3, 4, 5, 6S/m).

Effect of biofouling coverage

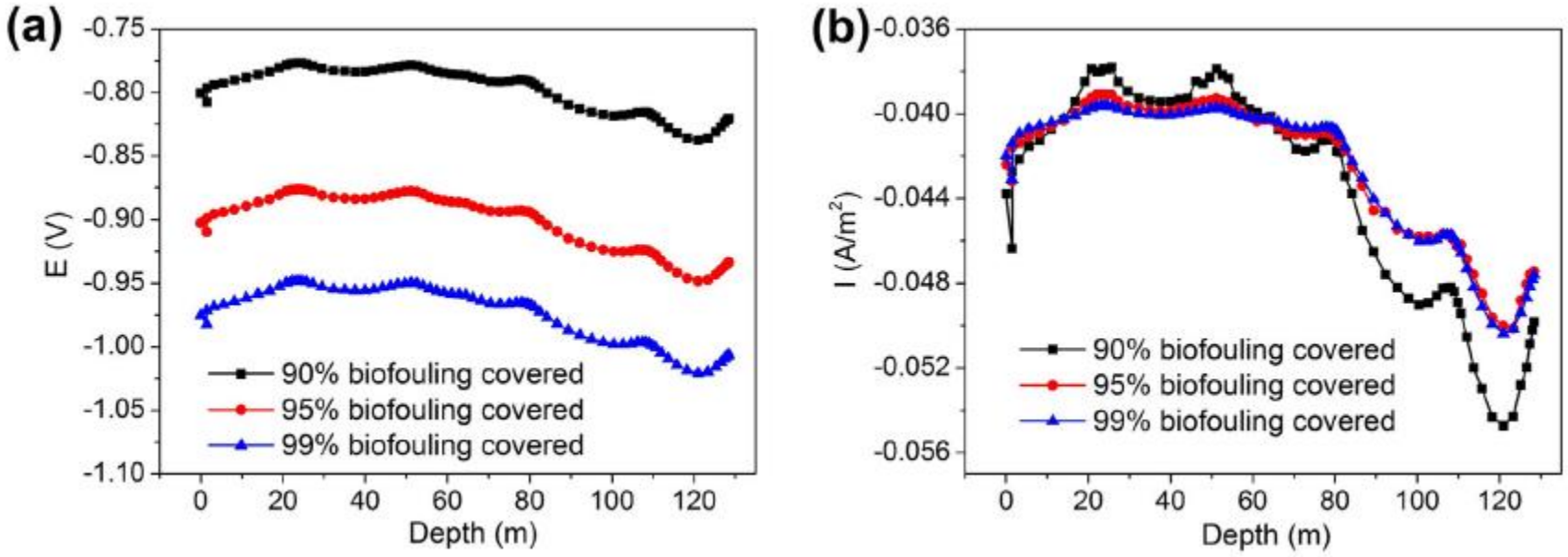

FIGURE 7 Calculated potential and current density distributions of Leg A-1 covered with 99, 95, and 90% biofouling, respectively.

Conclusions

- The off shore platform protected by ICCP was simulated by a 3-D FEM considering the influences of output current, anode location, seawater conductivity, and biofouling coverage rate.
- Biofouling inhibits the corrosion factors transport from seawater to steel structures.
- FE-SEM, EDS: magnesium oxides, biofouling deposits, and products of steel were doped with calcium oxides in the formation of calcareous deposit.

Conclusions

- FEM numerical model: An economical and effective ICCP system of a two anode ICCP was established.
- The ROV data monitored the potential distribution of the platform legs that well agreed with FEM calculated data.
- Numerical simulation of CP was an effective method to optimize the CP re-design and save the cost of CP engineering.